Acta Fac. Pharm. Univ. Comen. LXI, 2014 (2), p. 1–11
ISSN 1338-6786 (online) and ISSN 0301-2298 (print version)
DOI: 10.2478/afpuc-2014-0010

DE GRUYTER OPEN

ACTA FACULTATIS PHARMACEUTICAE UNIVERSITATIS COMENIANAE

NEUTRONS IN STUDIES OF PHOSPHOLIPID BILAYERS AND BILAYER–DRUG INTERACTION. I. BASIC PRINCIPLES AND NEUTRON DIFFRACTION*

NEUTRÓNY V ŠTÚDIU INTERAKCIÍ LIEČIV S FOSFOLIPIDOVÝMI DVOJVRSTVAMI. I. ZÁKLADNÉ PRINCÍPY A NEUTRÓNOVÁ DIFRAKCIA

Original research article

Bělička M.,[✉1] Devínsky F.,[2] Balgavý P.[1,2]

[1]*Comenius University in Bratislava, Faculty of Mathematics, Physics and Informatics, Department of Nuclear Physics and Biophysics, Slovak republic* / *[1]Univerzita Komenského v Bratislave, Fakulta matematiky, fyziky a informatiky, Katedra jadrovej fyziky a biofyziky, Slovenská republika*

[2]*Comenius University in Bratislava, Faculty of Pharmacy, Department of Chemical Theory of Drugs, Slovak republic* / *[2]Univerzita Komenského v Bratislave, Farmaceutická fakulta, Katedra chemickej teórie liečiv, Slovenská republika*

Received October 6, 2014 , accepted November 3, 2014

Abstract In our paper, we demonstrate several possibilities of using neutrons in pharmaceutical research with the help of examples of scientific results achieved at our University. In this first part, basic properties of neutrons and elementary principles of elastic scattering of thermal neutrons are described. Results of contrast variation neutron diffraction on oriented phospholipid bilayers with intercalated local anaesthetic or cholesterol demonstrate the potential of this method at determination of their position in bilayers. Diffraction experiments with alkan-1-ols located in the bilayers revealed their influence on bilayer thickness as a function of their alkyl chain length.

Slovak abstract V našom článku poukazujeme na viacero možnosti využitia neutrónov vo farmaceutickom výskume na príkladoch vedeckých výsledkov, ktoré sme získali na našej univerzite. V tejto prvej časti popisujeme základné vlastnosti neutrónov a elementárne princípy elastického rozptylu tepelných neutrónov. Výsledkami neutrónovej difrakcie na orientovaných fosfolipidových dvojvrstvách s interkalovaným lokálnym anestetikom alebo cholesterolom demonštrujeme potenciál tejto metódy pri určení ich lokalizácie v dvojvrstvách. Difrakčné experimenty s alkán-1-olmi lokalizovanými v dvojvrstvách odhalili ich vplyv na hrúbku dvojvrstvy ako funkcie dĺžky alkylového reťazca.

Keywords *neutron diffraction, phospholipid bilayer, local anaesthetic, alkan-1-ols, cholesterol*

Kľúčové slová: *neutrónová difrakcia, fosfolipidová dvojvrstva, lokálne anestetikum, alkán-1-oly, cholesterol*

INTRODUCTION

The results we describe were obtained in experiments performed at nuclear reactors in several neutron research centres. Most of our results come from the Léon Brillouin Laboratory (LLB, Saclay, France), the Joint Institute for Nuclear Research (JINR, Dubna, Russia), Budapest Neutron Centre (BNC, Budapest, Hungary) and Helmholtz Centre Berlin (HZB, Berlin, Germany). Recently, we used also the most powerful reactor source of neutrons for scientific purposes at the international Institut Laue-Langevin (ILL, Grenoble, France), in which Slovakia is a scientific member of the Central European Neutron Initiative Consortium (CENI) together with Austria, the Czech Republic, and Hungary. Further development of nuclear reactors, however, is currently limited by technological constraints associated with the transfer of heat generated by the nuclear chain reactions. Intensive efforts are therefore focusing on the development of new, even more powerful neutron sources. These include the European Spallation Source (2014), which is being built in Lund in Sweden.

BASIC PRINCIPLES

This chapter is based on texts written predominantly for physicists (Bacon, 1962, Feigin & Svergun, 1987, Pynn, 1990, Florek, 1992, Belushkin, 2010, Belushkin *et al.* 2011). Our aim here is

** Dedicated to Doc. Dr. Martin Bútora, PhD. on the occasion of his 70th birthday.*

** belicka.michal@gmail.com*

to present the basic principles in as simple a way as possible to make them understandable to the students of pharmacy at our university.

Neutrons are particles that, together with protons, form nuclei of all the known chemical elements and determine their physical properties. Free neutrons outside of atomic nuclei are unstable particles with half-life 10 min 11 s. They decay through β-decay into a proton, an electron, and an electron antineutrino, sometimes accompanied by γ-radiation. Their rest mass is very close to that of the proton ($m_n = 1.675 \cdot 10^{-27}$ kg). As all particles of non-zero mass, they display wave–particle duality, owing to which, depending on their state of motion, their particle or wave nature prevails. Their wave properties are characterised by wavelength λ given by the de Broglie relationship

$$\lambda = \frac{h}{p} = \frac{h}{m_n v}, \tag{1}$$

where h is Planck's constant and $p = m_n v$ is the momentum of neutron with velocity v. Neutrons have zero electric charge, thus do not interact with the electric field. Thanks to their zero charge, neutrons are not affected by electron shells, which is the cause of their high penetration ability into different materials. Neutron is further characterised by *spin* $s = ½$. As a result, neutrons, despite their zero total electric charge, are characterised by a nonzero magnetic moment given by the relationship

$$\vec{\mu}_n = -1{,}913 \frac{4\pi}{h} \mu_N \vec{s}, \tag{2}$$

where μ_N is the nuclear magneton and $\vec{s}$ is the neutron spin. The magnetic moment allows them to interact with a magnetic field. Experimentally, this feature is used for polarisation, that is, changing their spin/magnetic moment in the desired direction and orientation. Neutron polarisation has extensive experimental and practical use.

The total energy of neutrons consists predominantly of kinetic energy. If we consider neutrons in the absence of an electromagnetic field, then the energy of one neutron can be expressed as follows:

$$E = E_{kin} = \frac{p^2}{2m_n} = \frac{h^2}{2m_n \lambda^2}. \tag{3}$$

In practice, the energy of neutrons is often expressed through the thermodynamic temperature T, for which the following holds:

$$E = k_B T, \tag{4}$$

where k_B is the Boltzmann's constant. The assignment of the thermodynamic temperature to neutrons leads directly to their energy classification built on temperature-related concepts. Neutron scattering experiments aimed at examining biological structures most commonly employ thermal neutrons with energy 5 – 500 meV, velocity 10^3 – 10^4 m.s^{-1} and wavelength λ = 0.4 – 0.04 nm. By combining equations (3) and (4), we get a frequently used relationship between velocity and wavelength of neutrons

$$\lambda\,[\mathrm{nm}] = \frac{396}{v\,[\mathrm{m.s^{-1}}]} \tag{5}$$

Neutrons interact with material environment, that is, with atomic nuclei, predominantly through the so called strong nuclear interactions, one of the four fundamental forces of nature. Depending on the energy of the neutron and the particle, which it is incident on, different types of mutual interaction occur. In neutron scattering experiments, three kinds of reactions occur predominantly. At *elastic scattering*

$$\mathrm{n} + {}^{\mathrm{A}}_{\mathrm{Z}}\mathrm{X} \rightarrow \mathrm{n} + {}^{\mathrm{A}}_{\mathrm{Z}}\mathrm{X}, \tag{6}$$

there is no energy transfer between the incident neutron and the scattering particle and the sizes of the two particles' momenta are maintained. At *inelastic scattering*

$$\mathrm{n} + {}^{\mathrm{A}}_{\mathrm{Z}}\mathrm{X} \rightarrow \mathrm{n}' + {}^{\mathrm{A}}_{\mathrm{Z}}\mathrm{X}^*, \tag{7}$$

energy transfer between the incident neutron and the scattering particle does occur and not only the direction but also the sizes of the momenta of the two particles are changed. At *radiative capture*

$$\mathrm{n} + {}^{\mathrm{A}}_{\mathrm{Z}}\mathrm{X} \rightarrow {}^{\mathrm{A+1}}_{\mathrm{Z}}\mathrm{X}^*, \tag{8}$$

the incident neutron is captured by the atomic nucleus of the scattering particle, thus producing a new, energy-enriched isotope of the original element. The excited atomic nucleus then drops to a lower energy state by radiating a γ-quantum or a spontaneous nuclear decay occurs. All these three methods are used in pharmaceutical research. Elastic neutron scattering can be seen, for example, in neutron diffraction or small-angle neutron scattering; inelastic neutron scattering occurs in the neutron spin echo method. Radiative capture is used, for example, in *neutron activation analysis*, in which radiative neutron capture by the nuclei of the studied sample produces unstable isotopes.

Since in scattering experiments, the wave nature of moving neutrons is employed, it is quite natural to characterise them using variables describing waves – the *wave vector*

$$\vec{k} = \frac{2\pi}{\lambda} \vec{n}_0, \tag{9}$$

where $\vec{n}_0$ is a unit vector of the same direction and orientation as the momentum of the neutrons, and the *amplitude of the wave function* $A_{\vec{k}}(\vec{r}, t)$, which is generally a complex number

and whose square of the module $\| A_{\vec{k}}(\vec{r},t) \|^2$ gives the probability of the occurrence of a neutron with the wave vector $\vec{k}$ at location $\vec{r}$ and at time *t*. Thermal neutrons used in scattering experiments in biological macromolecular systems have the wavelength of the order of hundred thousand up to a million times larger than the typical size of an atomic nucleus, as a result of which they disperse on them (except for the above-mentioned exceptions) as on points of no internal structure and thus symmetrically in all directions. The incoming neutron, characterised by wave vector $\vec{k}$ and described by the plane wave function, is scattered on a point atomic nucleus *M* and, scattered, leaves under an angle *a* characterised by a wave vector $\vec{k}'$. Overall change in the wave vector is indicated by the so-called *transferred momentum vector* $\vec{q}$

$$\vec{q} = \vec{k}' - \vec{k}. \tag{10}$$

If we consider elastic scattering of neutrons on an atomic nucleus, it holds that $k = k'$ and, for the size of the transferred momentum, we can write

$$q = \frac{4\pi}{\lambda} \sin(\theta) \tag{11}$$

where 2θ is the scattering angle of the neutron (Fig. 1). The *neutron scattering length b* is defined for the atomic nucleus. Its numerical value is given by the negative ratio of the amplitudes of the scattered and incident neutron wave

$$b = -\frac{A'}{A} \tag{12}$$

Its value depends on the nucleon composition of the atomic nucleus, that is, on the number of protons and neutrons in the scattering atomic nucleus. In the event that the atomic nucleus has a non-zero spin, it also depends on the mutual neutron/nucleus spin configuration. This means in practice that two isotopes of the same element often have very different scattering lengths, that is, they scatter neutrons with different intensity and therefore can be distinguished by means of neutron scattering. This is a very important specific feature of neutron scattering compared to X-ray scattering, whose scattering amplitude depends on the number of electrons in the atomic shell and thus does not distinguish between different isotopes of the same element. The said property of neutron scattering has wide applications in biologically oriented research, as the elements with the largest difference in scattering lengths of their isotopes include hydrogen with $b(^1_1\mathrm{H})$ = 3.7406 fm and $b(^2_1\mathrm{H})$ = 6.671 fm. This allows using, for example, a simple substitution of "light" water H_2O for "heavy" water ^2H2O or a mixture thereof, to change the scattering properties of the environment in which the studied biological structure is present and thus to emphasise or, vice versa, suppress some of its areas. Another alternative is specific labelling of individual functional groups by deuteration. An example of such applications in drug research will be demonstrated below. The values of the scattering lengths of individual isotopes do not increase with the atomic number of the atomic nucleus, as is the case with X-ray scattering. This allows using neutron scattering for the observation of biological structures with a high amount of hydrogen, which is not possible using X-ray scattering. In the case of atomic nuclei with a non-zero spin, *b* also depends on the mutual orientation of the spins of the atomic nucleus and of the neutron being scattered. Each isotope with a non-zero spin is thus characterised by two values of the scattering length – for mutually the same and opposite orientation of the spins of the nucleus and of the neutron. There is no exact theoretical expression describing the values of scattering lengths of individual isotopes – they need to be determined experimentally. Their current values can be found, for example, on the website of the National Institute of Standards and Technology (2014).

The degree of interaction for not only neutrons, but any particles or radiation, with a scattering object is its effective cross section corresponding to the particles being scattered.

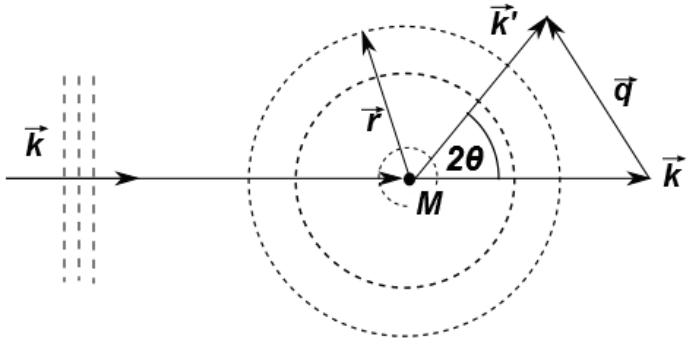

Fig. 1: Schematic representation of neutron scattering on a point-like scatterer. The incident planar neutron waves characterized by wave vector $\vec{k}$ are scattered on the point-like atomic nucleus M *in the form of spherical waves. Each scattered neutron is characterized by its scattering angle* 2θ*, wave vector $\vec{k}'$ and a corresponding vector of transferred momentum $\vec{q}$.*

For the effective cross section for thermal neutron elastic scattering on a single atomic nucleus, we have

$$\sigma = 4\pi b^2, \tag{13}$$

its size is most commonly expressed in units of 1 barn = 10^{-24} cm^2. In the case of several particles, the probability of scattering in different directions generally varies and therefore the so-called *differential effective cross section* $\frac{d\sigma(\alpha)}{d\Omega}$ is used, expressing the measure of neutrons scattered to the infinitesimal solid angle $d\Omega$. For example, in the case of small-angle neutron scattering, it takes the form of

$$\frac{d\sigma}{d\Omega}(\vec{q}) = \frac{k'}{k} \| (\frac{2\pi m_n}{h^2}) \sum_j b_j e^{-i\vec{q}\cdot\vec{r}_j} \|^2, \tag{14}$$

where the summation index *j* runs over all irradiated atomic nuclei in the sample in positions $\vec{r}_j$. The total effective cross section is obtained by integrating the above expression over the entire solid angle. Since the samples studied by means of neutron scattering contain on the order of 10^{23} particles, direct summation in equation (14) is not practically possible. Integration over the irradiated volume is therefore adopted, introducing a very practical quantity – *scattering length density* – ρ

$$\rho = \frac{\sum_k b_k}{\Delta V}, \tag{15}$$

where the summation runs over all atoms with scattering lengths b_k, which are present in volume ΔV. Expression (14) takes the form

$$\frac{d\sigma}{d\Omega}(\vec{q}) = (\frac{2\pi m_n}{h^2})^2 \| \int \rho(\vec{r}) e^{-i\vec{q}\cdot\vec{r}} d^3\vec{r} \|^2, \tag{16}$$

where integration takes place over the entire irradiated volume again. As implied by their nature, biological samples used in neutron scattering most often have the form of biomacromolecules or their aggregates contained in aqueous solutions. This fact simplifies the calculation of the integral in the relationship (16). If, in fact, we subtract, from function $\rho(\vec{r})$, the value of the scattering length of the water medium containing the studied molecular aggregates, we get the so-called *contrast scattering length density*

$$\Delta\rho(\vec{r}) = \rho(\vec{r}) - \rho_w, \tag{17}$$

where ρ_w is the scattering length density of the water medium. $\Delta\rho(\vec{r})$ is non-zero only in the places, where there are the examined macromolecules, but is zero at all points elsewhere. The overall result will include a so-called δ-function with the centre at the beginning, which does not affect the measured values of intensity. In the calculation of the estimated model of scattered neutrons intensity, which is directly proportional to the total effective cross-section, it is therefore sufficient to calculate the integral in expression (16) only over the volume of the molecules, which greatly facilitates the calculation. The above also implies that for a given system studied, the total measured neutron scattering intensity depends on the difference in the densities of scattering lengths of the various parts of the macromolecules and their aggregates, and of the aqueous medium, which, however, can be varied easily by changing the content of ^2H_2O. It is supposed that such changes in the composition of aqueous medium have no significant impact on the structure of the investigated systems.

The total intensity of scattered neutrons in each neutron experiment can, in principle, be divided into two components – *coherent* and *incoherent*. The coherent scattering component, as the name implies, is caused by the interference/combination of scattered wave functions at particular atomic nuclei, as a result of which the size generally varies with the change of $\vec{q}$, that is, different in various directions and depends on the wavelength/velocity of the neutrons. Conversely, incoherent neutron scattering, at any wavelength, always has the same intensity in all directions and contains no information about the internal structure of the examined system. Incoherent scattering in neutron experiments on biological samples is always present and has two essential components. The first is due to the presence of several isotopes of the same element in the irradiated system (due to the isotope dependence of *b*) and the second is due to the different orientation of the spins of isotopic nuclei with a nonzero spin and of the neutrons being scattered (due to the spin dependence of the scattering length *b*). And it is particularly the spin component of incoherent scattering that contributes significantly to the overall scattering in the case of biological samples, due to the high content of 'light' hydrogen atoms ($^1_1\mathrm{H}$). This is because the effective cross section of its incoherent scattering is more than 40 times larger than its coherent cross section.

NEUTRON DIFFRACTION

The first method employing thermal neutrons, which we will discuss, is neutron diffraction. Its basic principle is identical with that of light diffraction on a crystal – neutron waves pass the irradiated crystal and scatter on the individual atomic nuclei. The scattered waves interfere with each other and, depending on the periodically repeated structures present, give higher intensities (on the order of magnitude) at particular values of transferred momentum $\vec{q}$, so-called *Bragg's peaks*. By analogy from optics, it is known that this effect occurs when the path difference between the scattered waves is an integer multiple of their wavelength, that is, if the following is true:

$$n\lambda = 2d\sin(\theta), \tag{18}$$

where *n* is an integer, λ is the wavelength of the neutrons, *d* is the minimum distance between periodically repeated struc-

tures in the direction of the transferred momentum $\vec{q}$ and Θ is the angle between the incident neutron beam and the planar surface of a crystal. As the first observable peak, the first-order maximum is always detected, since the zero-order maximum lies in the direction of the incident neutron beam. For the size of the transferred momentum we have

$$q = \frac{4\pi}{\lambda}\sin(\theta). \tag{19}$$

The order of the intensity maximum is characterised by means of the absolute value of the respective *n*. At our Faculty of Pharmacy, we are engaged primarily in interactions of biologically active molecules with model biomembranes in the form of lipid bilayers of different composition. In neutron diffraction, these are either in the form of a large number of *oriented* bilayers stacked on a hydrophobic (Si, Au) or hydrophilic planar substrate (SiO_2) with varying degrees of hydration, or as an aqueous dispersion of *non-oriented* bilayers in multilamellar liposomes, including regions of different dominant orientation of the bilayers.

The oriented samples, in fact, form a one-dimensional crystal, in which a primitive cell formed by a bilayer, or possibly also by a part of the aqueous medium between the layers, is repeated in the direction of a normal to the plane of the bilayers with periodicity *d*. The normal thus indicates the only possible direction of transferred momenta $\vec{q}$, at which the intensity maxima are observed. When using a neutron beam of the same wavelength, in which case it is necessary to vary the direction of the incident neutron beam on the sample in order to change the range of detected $\vec{q}$, to obtain the required plot of intensities over the required range of $\vec{q}$ it is sufficient to change the orientation of the sample only by rotation about an axis perpendicular to the incident neutron beam and to the normal to the plane of the bilayers. In the case of non-oriented layers, similar arrangement of the bilayers does not occur throughout the sample but only locally, in limited areas. Nevertheless, it is possible to observe Bragg diffraction in this case as well. The position of the intensity maximum with the lowest corresponding value of *q* is, on the basis of (18), given by the relationship

$$d = \frac{\lambda}{2\cos(\theta_{max})} \tag{20}$$

where *d* is the already mentioned periodicity of bilayers, θ_{max} is the angle that corresponds to the maximum observed and that allows obtaining, through neutron diffraction, information on the structure of the investigated bilayers even in a non-oriented sample.

Oriented samples, due to their prevailing orderliness in the total volume, allow examining the internal structure of the bilayers themselves. The observed intensity of scattered neutrons is directly proportional to the square of the amplitude of the resulting scattered neutron wave *A(q)*

$$I(q) = \|A(q)\|^2, \tag{21}$$

which in this case is characterised by the size of transferred momentum *q*. If we do not consider multiple scattering of neutrons, which is negligible due to the sample size and the studied interval of the angle *Θ*, then the resulting amplitude of the scattered neutron wave is given by the Fourier transform of the density of the neutron scattering length *ρ(z)* in the direction of the normal to the plane of the bilayers *F(q)*, which is referred to as its *form factor*. Since individual bilayers have the same composition and hydration, they have the same internal structure, with the result that *ρ(z)* is a periodic function with period *d* and its Fourier transform has the form of the sequence $\{F(j)\}_{j=0}^{\infty}$. Moreover, the studied lipid bilayers are symmetrical with respect to their centre and therefore their Fourier transform contains only cosine members

$$\rho(z) = \frac{2}{d}\sum_j F(j)\cos(\frac{2\pi jz}{d}). \tag{22}$$

Member *F(j)* is called *the jth order diffraction form factor* and the integral *j*th order maximum intensity is I_j. The overall frequency of the corresponding jth maximum is given by the square of its amplitude $I_j = \frac{\|F(j)\|^2}{C_j}$, where C_j is the so-called Lorentz factor, which in the case of oriented bilayers is directly proportional to *j* (Nagle and Tristram-Nagle, 2000). The symmetry of the bilayer also implies that individual members *F(j)* are real numbers whose absolute value is given by the size of the observed maxima of scattered neutron intensities. Their sign is determined by observing the changes in individual intensities with varying scattering length density of the water medium – by *contrast variation*. Evaluation of changes in the intensity at the same time provides the correct normalisation of form factors important in the subsequent analysis. The linearity of the Fourier transform implies a significant fact that, in the case of systems consisting of several components, as is the case also with the lipid bilayers (lipid, water, dopant drug molecules), the form factor of the entire system is equal to the sum of individual components' form factors. Contrast variation thus becomes even more important, as it allows obtaining a scattering length density profile of the lipid bilayer in the absence of water. The correlation between the profile scattering length density *ρ(z)* and the form factors of the orders of the individual scattered neutron intensity maxima (22) provides means for obtaining a model-independent profile of bilayer's scattering length density, or also a possibility of creating its parameterised models and, through them, further evaluating experimentally obtained profiles $\Delta\rho(z)$.

Local anaesthetic

The aim of experiments in the paper by Balgavý *et al.* (1991) was to determine the location of the anaesthetic molecule at its intercalation into the phospholipid bilayer. Local anaesthetic [2-(ethyloxy)phenyl]-2-(1-piperidinyl)ethyl carbamate (abbreviation IV) was synthesised by Prof. Čižmárik at the Department of Pharmaceutical Chemistry, Faculty of Pharmacy, Comenius University in Bratislava as one homologue of the homologous series of heptacaine (Pešák *et al.*, 1980, Végh *et al.*, 2006). The deuterated anaesthetic with a radical $-OC_2D_5$ on the benzene ring (IV-D, Fig. 2) was prepared by Prof. J. Csöllei (FaF VFU Brno, 2014). The oriented samples were prepared on quartz slides as a mixture of dipalmitoyl phosphatidylcholine (DPPC) and the anaesthetic in a 1 : 1 molar ratio and hydrated by water vapour with 97 % humidity. The samples consisted of two series – with the anaesthetic IV and the anaesthetic IV-D. Three samples with different content of ^2H_2O (0 %, 50 %, and 100 %) were prepared for both mixtures and measured at a temperature of 23°C.

In the first step, oriented samples were analysed to determine the location of the deuterium-labelled ethyloxy groups on the normal of the bilayer. Given the thermal motion of molecules in the membrane, they were described by Gaussian distributions with the same standard deviation $\nu/\sqrt{2}$ and symmetrically placed at a distance of z_0 from the centre of the bilayer, that is, their contribution to the overall scattering length density has the form

$$\rho_M(z) = t_N\{\exp(-\frac{(z-z_0)^2}{\nu^2}) + \exp(-\frac{(z+z_0)^2}{\nu^2})\} \qquad (23)$$

with the corresponding component model form factor

$$F_M(j) = 2t_N \exp\left[-\frac{\pi^2\nu^2 j^2}{d^2}\right]\cdot\cos(\frac{2\pi h z_0}{d}), \qquad (24)$$

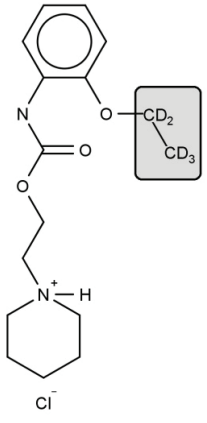

Fig. 2. Structural formula of a local anaesthetic IV-D, ([2-(ethylxy) phenyl]-2-(1-piperidinyl)ethyl carbamate), located in a DPPC bilayer. The grey box indicates the area of deuterium labelling. DPCC: dipalmitoyl phosphatidylcholine

where t_N is their scattering length density. The value of the position z_0 was determined by minimising the *R*-factor

$$R = \sum_i \frac{||F(j)| - F_M(j)|}{|F(j)|}. \qquad (25)$$

First, the form factors obtained were analysed. The variation of contrast was then evaluated and, using the linearity of the Fourier transform, the water component form factor was determined, enabling to obtain component form factors of the lipid bilayers with the normal and deuterium-labelled anaesthetic. Using relationship (22), their scattering length distributions on the normal of the bilayer were obtained (Fig. 3). The effect of deuterium labelling of the anaesthetic on the scattering length density profile of the bilayer is clearly visible. After their mutual subtraction, the obtained difference clearly illustrated the complicated distribution pattern of the anaesthetic in the DPPC bilayer. Most surprising was the finding that the difference shows the presence of two local maxima on either side of the bilayer, rather than one. It could be described using a pair of Gaussian distributions with centres at a distance z_0 = 1.28 nm and z_0 = 2.18 nm from the centre of the bilayer and with a standard deviation of 0.08 nm. This implies that the anaesthetic at a molar ratio of 1 : 1 in the DPPC bilayers is in two significant positions – in the first one, it is completely inserted in the area of hydrocarbon chains of DPPC with the aromatic ring located at the level of the carbonyl group of DPPC, and in the other, by contrast, all of its volume is located in the hydrophilic region of the DPPC bilayers, where it is horizontally oriented. This result is important when considering how the anaesthetic can interact at the level of a bilayer, for example, with various membrane proteins (receptors, ion channels).

Cholesterol

The neutron diffraction method also significantly helped in locating cholesterol in biomembranes. This work was significantly contributed to by Dr. Norbert Kučerka from the Department of Physical Chemistry of Drugs of our Faculty of Pharmacy. In the first series of experiments, Harroun *et al.* (2006) measured neutron diffraction on oriented lipid bilayers consisting of lipids with different numbers of unsaturated bonds in the hydrocarbon chain (16:0–18:1PC, di18:1PC, 18:1–20:4PC and di20:4PC) containing 10 mole percent of cholesterol. In order to determine the position of cholesterol in the lipid bilayer, samples were prepared for each lipid containing normal cholesterol and samples containing cholesterol labelled with deuterium in the area of the hydroxyl group (Fig. 4A). Scattering length density profiles of the lipid bilayer of the corresponding samples differed only as a result of the deuterium label, as the structure was otherwise the same. The phases of the individual form factor orders were determined differently from the previous example. Hydration was carried out using water with 8% ^2H_2O, of which the scattering length density ρ_w equals zero. Since for the zero order form factor we have

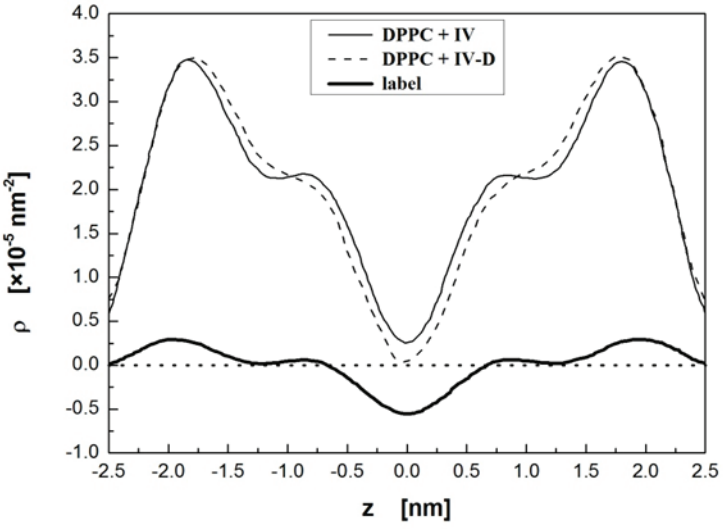

Fig. 3. Scattering length density profiles of lipid bilayers without water, consisting of DPPC with added normal IV (thin solid line) and deuterium- labelled IV-D (dashed line) anaesthetics. The thick solid line shows their difference (5-fold magnification) due to the deuterium labelling of the ethyloxy group on the benzene ring of the anaesthetic molecule. Adapted from Balgavý et al. (1991). DPCC: dipalmitoyl phosphatidylcholine

$$F_0 = b_{total} = \int_{-d/2}^{d/2} \rho(z)dz, \qquad (26)$$

where the integration is over one (averaged) bilayer and the corresponding interlamellar water volume, at zero ρ_w, thus not only its size but, because of the scaling, also the sizes of all other form factors are contributed to only by the atomic nuclei of the lipid and of cholesterol. This makes it possible, by the simple scaling of a complete form factor (22), to determine the signs of form factors of individual orders *F(j)* . To exclude the possible influence of phase differences in the lipid bilayers of the individual samples on their structure, which would lead to undesirable variations in the scattering length profiles, two samples were prepared for each of the lipid and cholesterol types at different relative humidities of the external environment (84 % using KCl and 93 % using KNO_3). In fact, in the case of the gel phase, the internal structure of the lipid bilayer depends on the number of water molecules in the interlamellar space per lipid molecule. Any changes in the structure are immediately reflected on the form factors of individual orders and thus on the observed intensities. However, as shown by the observations, in none of the studied mixtures, a change in the hydration caused a change in the intensities associated with structural changes. The only effect of the increased hydration of the samples was a proportional decrease in individual intensities associated with the change in periodicity of the oriented bilayers; however, their structure was preserved and, in all the measured samples, a liquid–crystal phase was thus also confirmed. In the corresponding samples with the same lipid, the change in the scattering length density profile was associated only with the different labelling of cholesterol, as intended. The above-described procedure was used to determine form factors of individual orders from the measured intensities for the examined samples. The form factors were then used in equation (22) to obtain neutron scattering length density profiles for the lipid bilayers in the samples. Profiles corresponding to the same lipid and different cholesterols (deuterated and non-deuterated) were subtracted from each other to give the expected differences

$$\rho_{deut}(z) - \rho_{hydr}(z), \qquad (27)$$

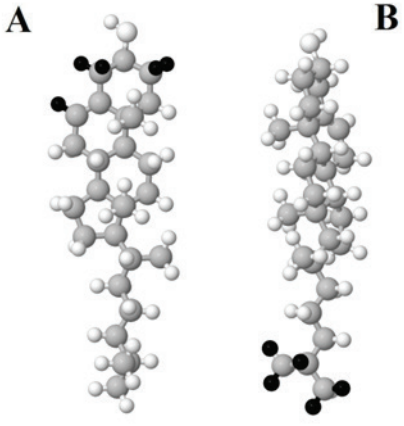

Fig. 4. Deuterium-labelled cholesterol molecules (black) used in its localisation in lipid bilayers using neutron diffraction method. A) Deuterium labelling in the area of the polar moiety containing a hydroxyl group –OH [2,2,3,4,4,6-$^2H_6$]. B) Deuterium labelling at the end of the hydrophobic hydrocarbon chain

where $\rho_{deut}(z)$ is the scattering length density profile of the bilayer with deuterated cholesterol, $\rho_{hydr}(z)$ is that with normal cholesterol, and z is the position on the normal of the bilayer with a centre in the middle of it. They are illustrated in Fig. 5. The evaluation was conducted using weighted fits by a pair of symmetric Gaussians if two peaks were present or by one Gaussian if only one peak was present. The obtained differences oscillate around the expected Gaussian distributions, which is a consequence of incomplete form factors (finite number of observed intensities), from which the scattering length profiles were constructed. Nevertheless, the differences obtained suggest a clear conclusion – the position of the hydroxyl group of cholesterol in the lipid bilayer depends on its composition, in this case also on the amount of unsaturated bonds present. However, the question of the general orientation of the cholesterol molecule in the lipid bilayer remained unresolved.

The answer was found by Harroun *et al.* (2008) in an analogous experiment, which, however, uses cholesterol with deuterium labelling at the end of its hydrocarbon chain which is hydrophobic (Fig. 4B). Similarly, as observed in the paper of Harroun *et al.* (2006), they obtained differences of scattering length density profiles in bilayers formed of dioleoylphosphatidylcholine (18:1 – 18:1 PC; DOPC) and diarachinoyl phosphatidylcholine (20:4 – 20:4 PC, DAPC) containing deuterium-labelled and normal cholesterol. Their plots are illustrated in Figs. 6A and 6B. As one can see, the end of the hydrocarbon chain, in both cases, is located only in the central region of the lipid bilayer, regardless of the number of unsaturated bonds present. The above implies a tendency of cholesterol to incorporate into the hydrophobic region of the lipid bilayers in parallel with saturated hydrocarbon chains or with those with low unsaturation, with its hydrophilic part in contact with the hydrophilic region of the bilayer, and, on the other hand, its repulsion to chains comprising a large number of unsaturated bonds, in which case it remains with the whole of its volume in the central part of the bilayer among the terminal methyl groups of hydrocarbon chains. Later, Kučerka *et al.* (2010a, 2010b) used neutron diffraction and cholesterol with deuterium labelling of the polar region (Fig. 4A) to investigate if the location of cholesterol in the central part of the bilayers formed by polyunsaturated lipids is stable or if it can be changed. The lipid bilayers were in the same liquid–crystal phase as was the case with the above-mentioned experiments, and contained 10 mole percent of normal and deuterium-labelled cholesterol, respectively. They were hydrated at a stable 84% relative humidity (using saturated aqueous solution of KCl) with water containing 8, 70, and 100% of ^2H_2O. To investigate the effect of the lipid bilayer composition on the location of cholesterol, two series of samples contained, in addition to DAPC, also palmitoyloleoylphosphatidylcholine (POPC) at 30 and 50 mole % and the third and fourth series of samples contained, in addition to DAPC, also 5 and 10 mole % of dimyristoylphosphatidylcholine (DMPC). For each lipid bilayer composition, the location of the deuterated polar moiety of cholesterol was determined as in the previous experiments on the basis of the four observed diffraction peaks. A graphic representation of the resulting findings can be seen in Fig. 7. Kučerka *et al.* (2010a, 2010b) found that while in the case of POPC, to change the position of the intercalated cholesterol in the centre of a DAPC bilayer into a position parallel to its chains, it is necessary to increase its content in the bilayer to more than 50 mole %; in the case of DMPC, the same effect can be achieved with a concentration of merely about 5 mole %. The cause of this fact appears to be related to the preferred formation of the cholesterol-saturated hydrocarbon chain aggregate, as shown graphically in Fig. 7. Also the latter results thus clearly confirm the repulsion of cholesterol to (poly)unsaturated lipid chains and, conversely, a strong attraction to fully saturated hydrocarbon chains.

These results will undoubtedly influence perceptions about the role of cholesterol and polyunsaturated lipids in membranes. In fact, all previous biological concepts were based on the results of experiments with bilayers of saturated or at most monounsaturated lipids.

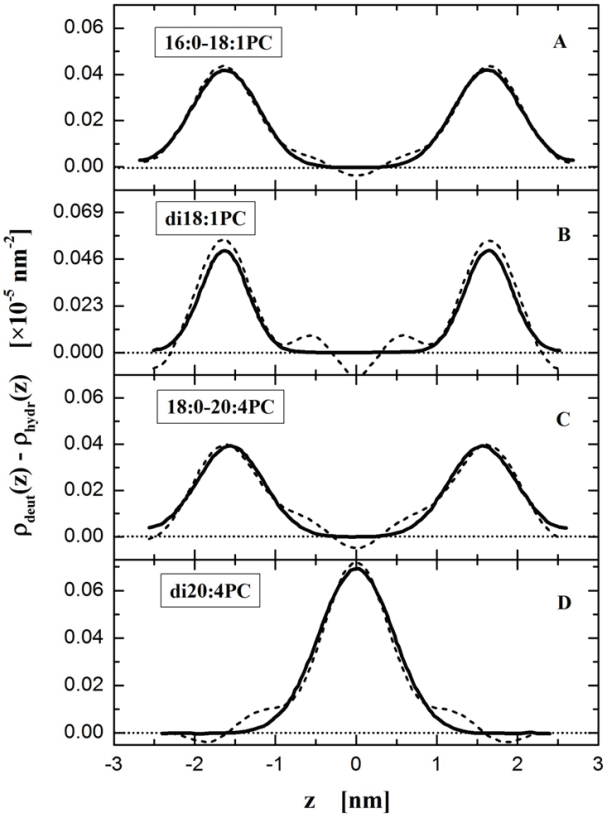

Fig. 5. Differences of the neutron scattering length density profiles of the investigated lipid bilayers containing normal cholesterol ($\rho_{hydr}(z)$) and cholesterol labelled with deuterium in the area of the hydrophilic moiety ($\rho_{deut}(z)$) (dashed line). The solid line indicates the weighted fit through a pair of symmetric Gaussians or one Gaussian. Adapted from Harroun et al. (2006)

General anaesthetics

It is known for several decades that the general anaesthetic potency of primary aliphatic alcohols (abbreviation CnOH,

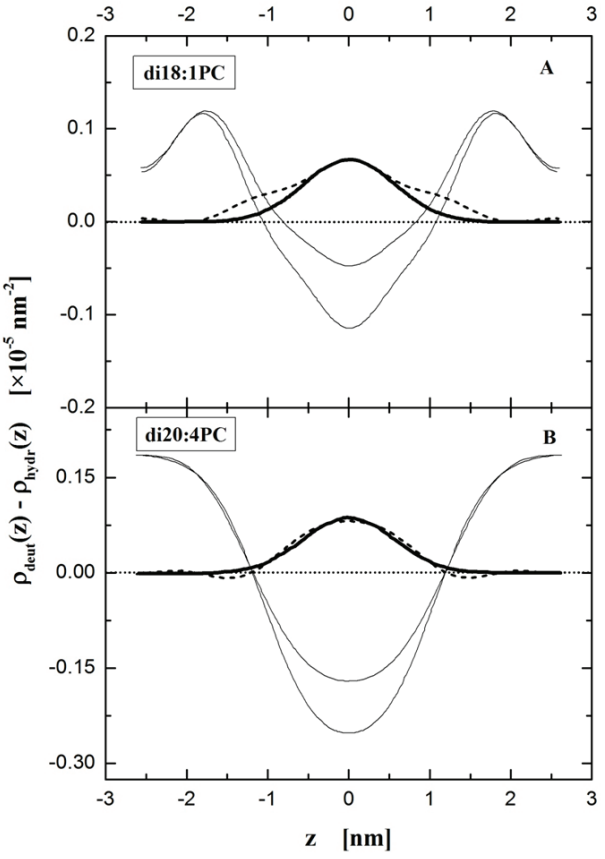

Fig. 6. Differences (dashed solid lines) of the neutron scattering length density profiles (thin solid lines) of the lipid bilayers containing cholesterol with deuterium-labelled terminal hydrocarbon chain and normal cholesterol. A) Lipid bilayers formed by DOPC (18:1- 18:1 PC). B) Lipid bilayers formed by diarachidonoylphosphatidylcholine (20:4- 20:4 PC). The thick solid line represents a weighted Gaussian fit. Adapted from Harroun et al. (2008). DOPC: dioleoylphosphatidylcholine

n is the number of alkyl carbon atoms) increases up to C11OH and then decreases, compounds longer than C13OH are non-anesthetic, that is, the homologous CnOH series displays a cut-off in the anaesthetic potency (Meyer and Hemmi, 1935, Pringle *et al.*, 1981). Cut-off effect was explained theoretically using a mathematical model 20 years ago in the paper of Cibula *et al.* (1994). The model was based on concepts summarised in a review article by Balgavý & Devínsky (1996), according to which the quasi parabolic dependence of biological activity in homologous series of amphiphilic compounds with linear hydrophobic substituents could be caused by a combination of partition equilibria and elimination of free volume below the hydrophobic substituent, which is usually shorter than phospholipid hydrocarbon chains in biomembranes. The theory predicts that at a constant CnOH concentration in the phospholipid bilayer, the bilayer thickness should be smallest for the shortest CnOH and that should increase with the alkyl chain length n. This prediction was put under test in neutron diffraction experiments done by Petrenko *et al.* (2010). They prepared multilamellar liposomes composed of fluid DOPC bilayers containing CnOH (with $n = 8, 10, 14, 16, 18$) at CnOH : DOPC = 0.3 molar ratio and hydrated with heavy water at $20.2 \geq D_2O$: DOPC ≥ 14.4 molar ratio. The bilayer thickness d_L calculated from the lamellar repeat period d using molecular volumes of DOPC, CnOH and D_2O, increased with the CnOH chain length n at CnOH : DOPC = 0.3 molar ratio linearly as expected: $d_L = (3.888 \pm 0.066) + (0.016 \pm 0.005) \cdot n$ (in nm).
The effect of CnOHs on the structure of oriented fluid bilayers prepared from DOPC was studied too. Oriented samples at CnOH : DOPC = 0.3 : 1 molar ratio (where n=10, 12, 14, 16) were prepared on quartz plates by a 'rock and roll method' (Tristram-Nagle, 2007). The same samples were used for neutron diffraction at low hydration (relative humidity 98%, contrasts 8%, 20% and 50% ^2H_2O) as well as in excess of water (100% ^2H_2O). The kinetics of hydration from gas phase was rather long (around 24 h). The distance of peaks d_{PP} across the bilayer in profiles of scattering length density such as in Fig. 3 was used as a measure of bilayer thickness. They have found that shorter alcohols (n=10, 12) decrease the spacing of DOPC bilayers while the longer (n=16) caused the increase of spacing at low hydration. A superposition of two different bilayers was observed in the presence of C18OH in DOPC. The effect of CnOH on the bilayer spacing was much smaller at excess of water, but the expected influence of CnOH on bilayer thickness was seen in this system too.

CONCLUSION

The neutron diffraction method has an important position in the study of lipid bilayers, because it provides a model-independent insight into the internal structure of lipid bilayers, but also has limitations. The main limitation is the condition of a repeating planar structure. Although neutron diffraction can also be used for partially oriented samples, in which the aforementioned repetitive planar structure is always present in smaller delimited areas, it cannot be practically used to investigate the internal structure of the bilayers in such cases. Since an essential condition for the use of neutron diffraction is a periodically repeating identical structure in the sample, the use of neutron diffraction to study the influence of dopant biomolecules or drugs on a lipid bilayer is limited to molecules that intercalate into the bilayer with their whole volume and do not affect the adjacent bilayers. Neutron diffraction is therefore not a suitable method, for example, to study membrane proteins, the dimensions of which often several times exceed the thickness of the bilayer.

ACKNOWLEDGEMENTS

This publication is the result of the project implementation: Center of Excelence in Security Research ITMS code: 26240120034 supported by the Research & Development Operational Programme funded by the European Regional Development Fund (ERDF). This work was supported by the Slovak Research and Development Agency under the contract No.

APVV-0516-12, by the VEGA grants 1/0159/11 and 1/0785/12, and by the JINR project 07-4-1069-09/2011. PB thanks Professor Tolya Balagurov (Frank Laboratory of Neutron Physics, Joint Institute of Nuclear Research, Dubna, Russia), Professor Valentin Gordeliy (now at the Centre of Biophysics and Physical Chemistry of Supramolecular Structures, Moscow Institute of Physics and Technology, Dolgoprudny, Russia and at Institut de Biologie Structurale, Grenoble, France) and Dr. Thomas Hauß (Institute for Soft Matter and Functional Materials, Helmholtz-Zentrum Berlin für Materialien und Energie, Berlin, Germany) for help with neutron diffraction experiments and for fruitful discussions. PB and FD thank their former and present students for their important contributions. MB thanks the Central European Neutron Initiative for an one-year scholarship and the staff of Large Scales Structure Group in Institute Laue-Langevin for help, discussions and hospitality.

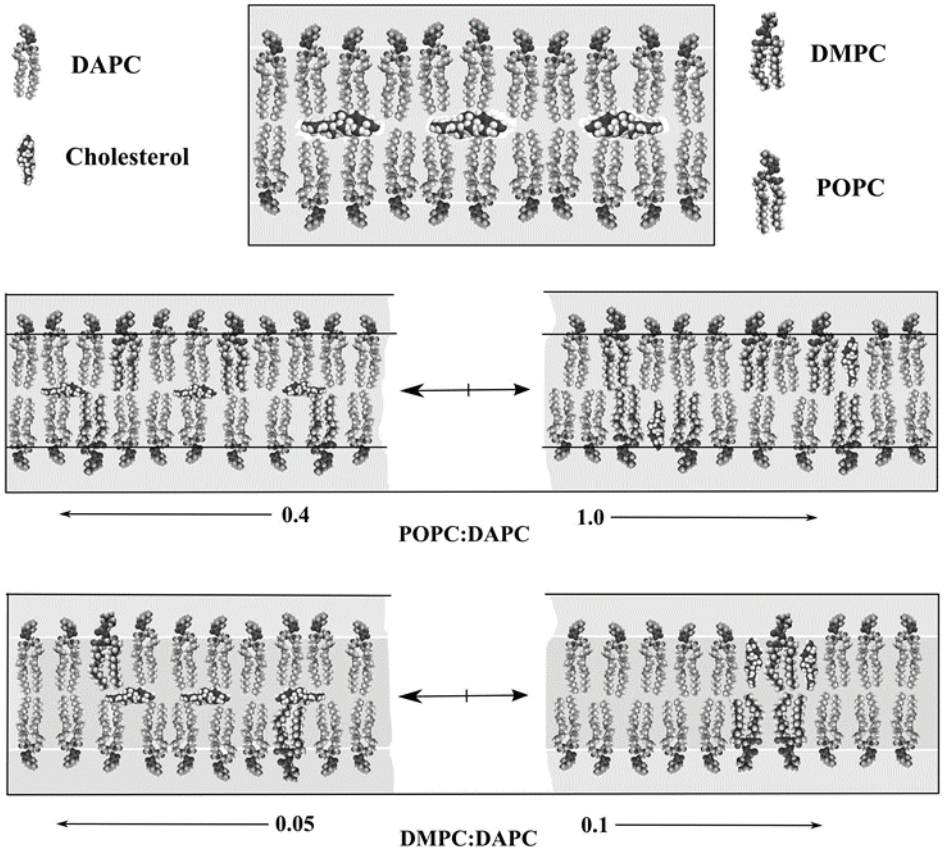

Fig. 7. Graphic representation of the output of neutron diffraction experiments investigating the influence of the composition of the lipid bilayer on the position of intercalated cholesterol. In the case of POPC (centre) it is necessary to increase the content of cholesterol in the DAPC bilayer above 50 mole percent in order to achieve integration of cholesterol among the lipid chains from the central part of the bilayer. For DMPC, the same effect can be observed at its concentrations in the DAPC bilayer from about 5 mole percent. Adapted from Kučerka et al. (2010). DAPC: dipalmitoyl phosphatidylcholine; DMPC: dimyristoylphosphatidylcholine; POPC: palmitoyloleoylphosphatidylcholine

REFERENCES

[1] Bacon GE. Neutron Diffraction, 2nd ed. Oxford: Clarendon Press; 1962.

[2] Balgavý P, Gordeliy VI, Syrykh AG. Influence of local anesthetic heptacaine hydrochloride and its derivatives on the structure of lipid membranes from dipalmitoyllecithin. JINR Commun. 1991;14-91-387:1–14.

[3] Belushkin AV. Fundamentals of Studies of the Properties of Condensed Matter using Neutron Scattering (in Russian). Dubna, JINR; 2010.

[4] Belushkin AV, Kozlenko DP, Rogachev AV. Synchrotron and neutron-scattering methods for studies of properties of condensed matter: Competition or complementarity? J Surface Invest. 2011;5: 828-855.

[5] Cibula J, Gallová J, Uhríková D, Balgavý P. Interaction of surfactants with model and biological membranes. IX. Theoretical model of the biological activity dependence on the hydrocarbon chain length (in Slovak). Čes Slov Farm. 1994;43:84-88

[6] Balgavý P, Devínsky F. Cut-off effects in biological activities of surfactants. Adv Colloid Interface Sci. 1996;66:23-63

[7] European Spallation Source. About ESS. Lund, Sweden: 2014. (http://europeanspallationsource.se/european-spallation-source). Accessed September 29, 2014.

[8] FaF VFU Brno. Prof. RNDr. Jozef Csöllei, CSc. Brno, Czech Republic: Faculty of Pharmacy, University of Veterinary and Pharmaceutical Sciences in Brno: 2014. (http://faf.vfu.cz/research-and-development/department-of-chemical-drugs/csollei.html). Accessed September 29, 2014.

[9] Feigin LA, Svergun DI. Structure Analysis by Small-Angle X-Ray and Neutron Scattering. New York, NY: Plenum Press; 1987.

[10] Florek M. Experimental Nuclear and Subnuclear Physics - Neutron Physics (in Slovak). Bratislava: Comenius University; 1992.

[11] Harroun TA, Katsaras J, Wassall SR. Cholesterol hydroxyl group is found to reside in the center of a polyunsaturated lipid membrane. Biochemistry. 2006;45:1227–1233.

[12] Harroun TA, Katsaras J, Wassall SR. Cholesterol is found to reside in the center of a polyunsaturated lipid membrane. Biochemistry. 2008;47:7090–7096.

[13] Kondela T, Gallová J, Hauss T, Balgavý P. The effect of 1-alkanols on the structure of DOPC model membrane. A small-angle neutron diffraction study. Poster presented at: 20th Conference of Slovak Physicists; September 2-5, 2013; Bratislava, Slovakia.

[14] Kučerka N, Marquardt D, Harroun TA, *et al.* Cholesterol in bilayers with PUFA chains: Doping with DMPC or POPC results in sterol reorientation and membrane-domain formation. Biochemistry. 2010a;49:7485–7493.

[15] Kučerka N, Nieh MP, Marquardt D, Harroun TA, Wassail SR, Katsaras J. Cholesterol in unusual places. J Phys Conf Ser. 2010b;251:012038.

[16] Meyer KH, Hemmi H. Beiträge zur Theorie der Narkose III. Biochem Z. 1935;277:39-72.

[17] Nagle JF, Tristram-Nagle S. Structure of lipid bilayers. Biochim Biophys Acta. 2000;1469:159–195.

[18] National Institute of Standards and Technology. Neutron Scattering Lengths and Cross Sections. Gaithersburg, MD: NIST Center for Neutron Research, 2014. (http://www.ncnr.nist.gov/resources/n-lengths/). Accessed September 29, 2014.

[19] Pešák M, Kopecký F, Čižmárik J, Borovanský A.: Study of local anesthetic. Part 70. Some physico-chemical properties of piperidinoethylesters of alkoxyphenylcarbamic acids. Pharmazie. 1980;35:150-152.

[20] Petrenko VI, Klacsová M, A.I. Beskrovnyy, Uhríková D, Balgavý P. Interaction of long-chain n-alcohols with fluid DOPC bilayers: a neutron diffraction study. Gen Physiol Biophys. 2010;29:355-361.

[21] Pringle MJ, Brown KB, Miller KW. Can the lipid theories of anesthesia account for the cutoff in anesthetic potency in homologous series of alcohols? Mol Pharmacol. 1981;19:49-55.

[22] Pynn R. Neutron Scattering – a Primer. Los Alamos, NM: Los Alamos Science, 1990. (http://fas.org/sgp/othergov/doe/lanl/pubs/00326651.pdf) Accessed September 29, 2014.

[23] Tristram-Nagle S. Preparation of oriented, fully hydrated lipid samples for structure determination using X-ray scattering. Methods Mol Biol. 2007:400;63-75.

[24] Végh V, Čižmárik J, Hahnenkamp K. Is there a place for local anesthetics structurally different from classical amid or ester local anesthetics? Curr Opin Anaesthes. 2006;19:509–515.